



American Society of
Mechanical Engineers

ASME Accepted Manuscript Repository

Institutional Repository Cover Sheet

Saeed

Izadi

First

Last

ASME Paper Title: **Investigating the Impact of Steam Enhancement on Combustion in a Swirl-Assisted Jet-Stabilized Gas Turbine Combustor**

Authors: **Saeed Izadi, Oliver Kislak, Jan Zanger, Hannah Seliger-Ost, Peter Kutne, Manfred Aigner**

ASME Journal Title: **Investigating the Impact of Steam Enhancement on Combustion in a Swirl-Assisted Jet-Stabilized Gas Turbine Combustor**

Volume/Issue: 147(1): 011001

Date of Publication (VOR* Online) **September 6, 2024**

<https://asmedigitalcollection.asme.org/gasturbinespower/article-abstract/147/1/011001/1203032/Investigating-the-Impact-of-Steam-Enhancement-on?redirectedFrom=fulltext>

ASME Digital Collection URL:

DOI: <https://doi.org/10.1115/1.4066235>

INVESTIGATING THE IMPACT OF STEAM ENHANCEMENT ON COMBUSTION IN A SWIRL-ASSISTED JET-STABILIZED GAS TURBINE COMBUSTOR

Saeed Izadi, Oliver Kislat, Jan Zanger, Hannah Seliger-Ost, Peter Kutne, Manfred Aigner

German Aerospace Center (DLR), Institute of Combustion Technology
Stuttgart, Germany

Email: saeed.izadi@dlr.de

ABSTRACT

A newly developed gas turbine combustor system based on the swirl-assisted jet-stabilized concept using Jet A-1 and natural gas as reference fuel is tested under wet conditions to evaluate its combustion characteristics in the presence of steam. The effect of steam injection into the gas turbine combustor under both spray and superheated liquid fuel injection conditions is studied experimentally on an atmospheric test rig. The experiments are conducted at atmospheric pressure and an elevated combustion air temperature of 305°C. To evaluate the effect of steam injection on combustion performance, the water-to-gas ratio (WGR) is varied from 0 to 32%. Even at very high WGR levels, the results show virtually no combustion thermoacoustic instability during operation. With increasing WGR = 0 to 16% and at stoichiometric condition, NO_x reductions of -82% to -100% were observed during Jet A-1 and natural gas combustion, respectively. It is shown that the reduction of the combustion zone temperature due to the steam acting as a heat sink is the main cause of the NO_x decrease. For both wet and dry conditions, CO levels remained fairly similar. Both flame length and flame height above the burner increased with increasing WGR. This is due to the reduced reactivity of the fuel-air mixture. The operating range of the burner remained fairly constant for Jet A-1 until WGR = 20%, while it decreased significantly with increasing WGR for natural gas combustion. While the effect of the WGR on CO was modest, the greatest effect of the WGR was on the heat release zone intensity at a constant air to fuel ratio. In reducing the NO_x levels of Jet A-1 and natural gas combustion, both thermal and chemical effects of steam injection were observed. However, steam acting as a heat sink and lowering the flame temperature, thereby reducing the thermal NO formation rate, was the dominant factor in NO_x reduction.

Keywords: Gas turbine, combustor, Liquid fuel, Jet A-1, OH* chemiluminescence, Dry Low-NO_x, Wet combustion, Compact flames, Steam Injection.

NOMENCLATURE

AFR _{stoich}	Stoichiometric Air to Fuel Ratio
CO	Carbon Monoxide
CO ₂	Carbon Dioxide
D _{AN}	Air Nozzle Diameter
D _{FT}	Flame Tube Diameter
FL	Flame length
GT	Gas Turbine
GT	Gas Turbine
H ₂ O	Steam / Water
HAB	Height Above Burner
IRO	Intensified Relay Optics
LBO	Lean Blowout
NG	Natural Gas
NO	Nitric Oxide
NO ₂	Nitrogen Dioxide
NO _x	NO + NO ₂
OH*-CL	Hydroxyl Radical Chemiluminescence
PLIF	Planar Laser-Induced Fluorescence
p _{sat}	Saturation Pressure
P _{th}	Thermal Power
s _L	Laminar Flame Speed
SN	Swirl Number
T _{ad}	Adiabatic Flame Temperature
T _{sat}	Saturation Temperature
UHC	Unburned Hydrocarbons
v _{bulk}	Bulk Velocity
WGR	Water-to-Gas Ratio
x	Radial Direction
y	Axial Direction
ΔT	Preheat Level of Fuel
λ	Air Equivalence Ratio
θ	Swirl Angle

1. INTRODUCTION

Economic justification and more stringent emission requirements have motivated many gas turbine (GT) engineers and scientists to search for methods to increase the efficiency of

the GT cycle and to reduce the emissions of pollutants. There are a few proposed methods that have been effective in the reduction of nitrogen oxides ($\text{NO}_x = \text{NO} + \text{NO}_2$) emissions. The first method is the dry low NO_x combustion. This is the most widely used method for reducing NO_x emitted in gas turbine combustors. Selective Catalytic Reduction (SCR) is the second method. The third method is catalytic combustion, which has been shown to significantly reduce NO_x emissions in GT combustors [1]. [2]

Emission control of GT engines requires precise adjustment of the fuel-air mixture ratio to avoid hot regions in the combustion chamber. A major driver of thermal NO formation is reaction zone temperature, and an effective NO suppression method is to inject more air into the reaction zone than required for stoichiometric combustion [3]. For this purpose, several concepts to dilute the fuel-air mixture and thus lower the flame temperature in the reaction zone have been proposed by many researchers [4–7], mainly based on lean-fuel combustion.

In terms of NO_x levels reduction, the advantages of dry low- NO_x combustion concepts as demonstrated by the literature [8–10] can also be achieved by wet combustion. Water or steam injection can be used in addition to the lean low NO_x concepts to further reduce NO_x levels or separately to minimize flame temperature and avoid thermal NO. The water-to-gas ratio (WGR: see Equation 1.1), which was previously used by [11], is a term that quantifies the amount of water or steam that is injected into the combustion zone:

$$WGR = \frac{\dot{m}_{\text{water}}}{\dot{m}_{\text{water}} + \dot{m}_{\text{air}}} \quad (1.1)$$

The addition of more air to the reaction zone will dilute the flame and lower the flame temperature, but it will also increase the velocity in the primary reaction zone, which will result in combustion stability problems. However, the injection of water or steam to a large extent avoids the velocity change problem while acting as a heat sink. [3]

The concept of wet combustion has been adopted in a number of stationary gas turbines, such as the GE MS7001E [12]. A new concept for a water-enhanced turbofan (WET) for aviation is presented in a study by Kaiser et al. [13]. Their paper provides a comprehensive description of the WET configuration and cycle. The concept uses the injection of superheated steam into the combustor to improve performance and emissions. The proposed cycle also achieves a 13% improvement in engine specific fuel consumption. The reduction in NO_x levels is claimed to be as high as 90%.

For the investigation of the technological feasibility of a new water enhanced gas turbine cycle, a mathematical model for a laboratory scale ground demonstrator was developed by Marcellan et al. [14]. The numerical results were used to formulate basic design principles, such as potential pressure losses, for the test rig. The test rig was built using the unmodified M250.

In a study by Degges et al. [15] on the influence of steam on the flammability limits of premixed natural gas/oxygen and steam mixtures, the role of steam injection on the chemistry of hydrocarbon-oxygen mixtures was characterized. The reactivity

of the mixture with a higher adiabatic flame temperature was suppressed by the steam. The researchers found that steam, which is highly efficient as the third body collision partner, significantly affected the chain-terminating reactions that lead to the combustibility threshold. Depending on the steam content, either the thermal effect (lowering the temperature) or the chemical kinetics effect (supporting the chain-terminating reactions) was dominant.

However, there are practical limitations to the use of water injection in gas turbine combustors. There is a penalty for the additional thermal energy (fuel) required to heat the injected water. This penalty can be avoided if waste heat from the exhaust gas is used to evaporate the water. Reduced combustor operating range due to water injection, increased carbon monoxide (CO) and unburned hydrocarbon (UHC) levels and increased thermoacoustic risk are some of the drawbacks reported in the literature [16].

Thorough investigation of dry low NO_x operation of the swirl-assisted jet-stabilized combustor discussed in this study is presented in separate work [17–19]. This study is concerned with characterizing the resistance to external disturbances of the swirl-assisted jet-stabilized combustor with dilution of the combustion air by inert gases such as steam. Additionally, the experiments will demonstrate that the combustor can operate with both liquid and gaseous fuels.

2. EXPERIMENTAL SETUP

For the experimental investigation of the developed combustor, the test facilities of the German Aerospace Center (DLR), Institute of Combustion Technology have been used. The newly developed combustor investigated in the experiments is a single-nozzle swirl-assisted jet-stabilized combustor with a concentric simplex pressure-swirl atomizer characterized thoroughly in [17–19]. In order to assess the effect of steam injection on the combustion performance of liquid fuel Jet A-1 Ref. 3 (see Table 1 for fuel surrogate composition and [20] for other fuel physical and chemical characteristics) and natural gas (as the reference fuel, see Table 1 for details of NG composition), experimental tests have been conducted on an optically accessible atmospheric test rig.

The purpose of the conducted experiments was to evaluate the effect of steam injection on the flame emissions, stability and shape. In addition, a better comparison with literature work can be made by testing with NG, since there is much research related to steam injection into NG/methane flames.

A commercially available simplex pressure-swirl atomizer (Feinzerstäuberdüse TD, manufactured by DIVA Sprühtechnik GmbH, Hamburg, Germany) with a flow number (FN_{US}) of 0.8 $[\text{lb/h}]/[\text{psid}]^{0.5}$ [21] and a spray angle of 80° at a pressure drop of 3 bar (water temperature of 20°C) was used for Jet A-1 atomization. The injection nozzle was made of austenitic steel EN 1.4305 (AISI 303). For the NG experiments, a $\varnothing 1.3$ mm plain-orifice injector was used as the fuel nozzle.

TABLE 1: JET A-1 SURROGATE [20] AND NATURAL GAS COMPOSITION OF STUTTGART AS OF JUNE 2023 MEASURED DURING THE EXPERIMENTS

Jet A-1 (Ref. 3)		
Component	Formula	%mol/mol
N-decane	n-C ₁₀	11.52
2-methyl decane	i-C ₁₁	22.54
N-propylcyclohexane	C ₉ H ₁₈	25.53
Decalin	C ₁₀ H ₁₈	15.61
Propylbenzene	C ₉ H ₁₂	15.45
Indene	C ₉ H ₈	1.53
Tetralin	C ₁₀ H ₁₂	5.78
Naphthalene	C ₁₀ H ₈	0.21
1-methylnaphthalene	C ₁₁ H ₁₀	1.63
Biphenyl	C ₁₂ H ₁₀	0.18
Acenaphthylene	C ₁₂ H ₈	0.01
AFR _{stoich}		14.62
Lower Heating Value	[MJ/kg]	43.14

Natural Gas (NG)		
Component	Formula	%mol/mol
Methane	CH ₄	91.120
Ethane	C ₂ H ₆	5.113
Propane	C ₃ H ₈	0.880
Iso-Butane	i-C ₄ H ₁₀	0.259
n-Butane	n-C ₄ H ₁₀	0.085
n-Hexane	n-C ₆ H ₁₄	0.166
Carbon dioxide	CO ₂	1.139
AFR _{stoich}		16.25
Lower Heating Value	[MJ/kg]	47.36

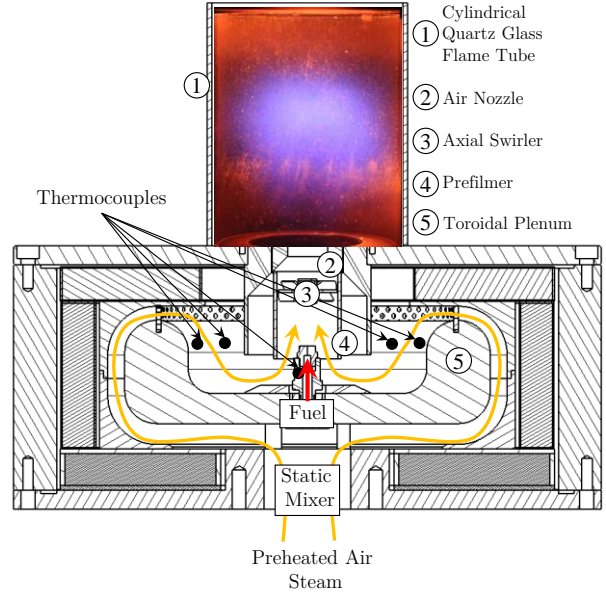


FIGURE 1: SECTIONAL VIEW OF THE TESTED COMBUSTOR

The general experimental set-up is illustrated in Figure 3. The air flowed to the combustor through a T-junction preheated by two electric heaters (15 kW_{el} each). The temperature of the preheated air was set to 305 °C. After passing through a mass flow controller (Cori-Flow, manufactured by Bronkhorst, Ruurlo, The Netherlands), another electric heater (3.6 kW_{el}) preheated the Jet A-1 for superheated fuel injection tests. Due to technical limitation described in Section 5, the fuel preheater was later used as water preheater to inject superheated steam into the air prior to the combustor. Water or steam was injected about 1000 mm from the combustor outlet using similar pressure-swirl injector used as for the Jet A-1 injection. The plenum contained the fuel lance and injector.

A sectional view of the combustor operated in this study is shown in Figure 1, where the preheated air and steam entered a toroidal plenum through a static mixer where they were evenly distributed before entering the combustor. The deflection of the air by the toroidal plenum is similar to the air flow path in a micro-GT combustor. Depending on the test requirements, Jet A-1 or NG was injected into a premix channel. The premix channel consisted of a prefilmer and an axial vane swirler (see [17] for detailed combustor description). The prefilmer and the swirler make a significant contribution to the improved atomization / vaporization of the liquid fuel (see [18] for detailed liquid fuel evaporation characterization of the combustor). A detailed overview of the combustor dimensions and the swirler geometry (swirl angle $\theta = 40^\circ$) is given in Figure 2 A and B, respectively.

Before exiting the air nozzle into the quartz glass combustion chamber, the preheated air and steam were mixed with superheated/sprayed Jet A-1 fuel or NG. To measure the average temperature of the incoming combustion air, four thermocouples (type N) were installed circumferentially in the plenum. One type N thermocouple was mounted on the fuel lance (12 mm prior to injector exit orifice) to measure the fuel temperature prior to injecting. The accuracy of the temperature measurement is $\pm 1.5^\circ\text{C}$, which reflects the accuracy of the calculated ΔT levels.

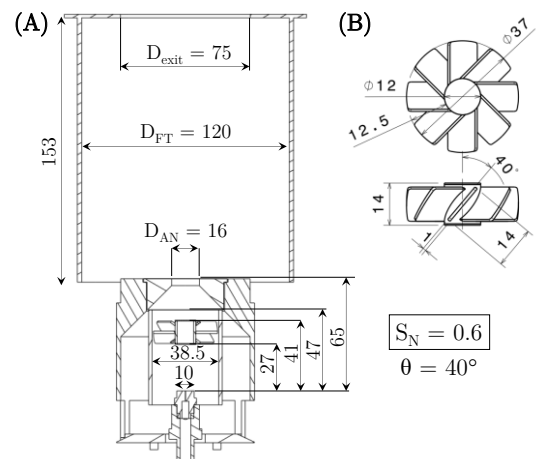


FIGURE 2: (A) DIMENSIONS OF THE STUDIED COMBUSTOR, WITH AIR NOZZLE, FLAME TUBE AND (B) SWIRLER

A natural gas-fired afterburner was used to combust the unburned liquid fuel prior to ignition and after combustor

flameout. The hot (up to 900°C) exhaust from the natural gas burner was led into the combustion chamber above the quartz glass flame tube. The afterburner was turned off during all measurements of lean blowout limit, emissions, and OH* chemiluminescence. Concentric to the flame tube, a sample of the exhaust gas was taken 566 mm downstream of the front plate of the combustor at a rate of 47.5 L/min.

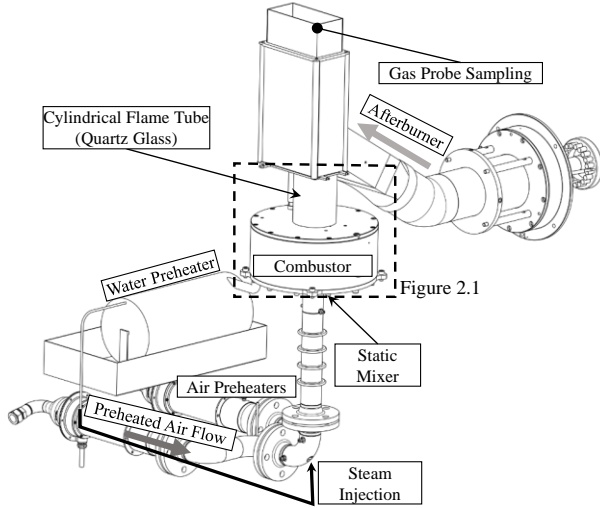


FIGURE 3: EXPERIMENTAL SETUP SCHEMATIC

3. SUPERHEATED INJECTION OF JET A-1

The concept of superheated injection of liquid fuel has the potential to reduce the length and residence time required for fuel to vaporize in the premixing chamber, thereby eliminating the risk of flashback and autoignition. An increase in fuel temperature may not only have the effect of NO reduction [22], but it may also have the effect of flame length reduction. The effect of fuel temperature on spray behavior was characterized in a study by Yin et al. [23] on superheated injection of liquid fuels. It was shown that while the magnitude of the superheating effect (see Equation 3.1) on the transition of the spray morphology from the mechanical break-up to the superheated regime was small, its significant effect on the jet-to-plume and fuel evaporation was quite visible. The liquid atomization behavior decreased at high fuel preheating, which explained the predominant thermal effect on spray morphology.

Comprehensive investigation of the currently used Jet A-1 and three other liquid fuels in spray and superheated conditions is conducted in a separate paper [19].

The level of superheat (ΔT) (see Equation 3.1) is a commonly used parameter associated with the superheated injection (flash boiling) [24]. This parameter describes the difference between injected fuel temperature T_{fuel} and its saturation temperature T_{sat} at the backpressure p_{∞} (combustion chamber pressure).

$$\Delta T = T_{fuel} - T_{sat}(p_{\infty}) \quad (3.1)$$

The saturation temperature T_{sat} of the fuel Jet A-1 used in the current study was calculated using the Antoine Equation 3.2 [25,26], where, p_{sat} is the saturation pressure in [Pa]:

$$T_{sat} [K] = \frac{4264.57763}{21.3176792 - \ln p_{sat}} + 43 \quad (3.2)$$

The resulting T_{sat} at 1 atm (1.01325 bar) is 478.5 K ($\approx 205^{\circ}\text{C}$).

4. Measurement techniques

For the current steam injection experiments, two main combustion diagnostic techniques were utilized: OH* chemiluminescence and exhaust gas analysis.

4.1 OH* Chemiluminescence

The formation of reactive species in the combustion zone is the result of the energetic ground state species. The lifetimes of these excited species are short. In a process known as luminescence, they emit energy in the form of light. When this luminescence is caused by chemical excitation rather than thermal excitation, it is called chemiluminescence. The intensity of chemiluminescence depends on the chemical composition and is less affected by temperature. In hydrocarbon flames, OH* and CH* give rise to the strongest chemiluminescence. [27,28]

Figure 4 shows the general measurement setup. In this case, the field of view of the OH*-CL is centered in the axial direction of the flame tube. This allowed the observation of the whole optical accessible flame tube. With an image resolution of 5 pixels per mm, the camera system was placed approximately 1500 mm from the combustor.

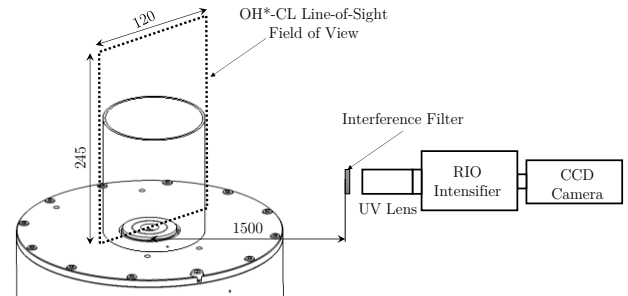


FIGURE 4: SCHEMATIC ILLUSTRATION OF OH*-CL LINE-OF-SIGHT MEASUREMENT SETUP

The OH* chemiluminescence (OH*-CL) intensities as a measure for global heat release zone [29] were recorded for all operating points using a charge-coupled device camera (LaVision Imager Pro Plus 2M, 1600 x 1200 pixels) in combination with an intensifier (LaVision: Intensified Relay Optics), a CERCO 100 mm UV lens F/2.8 and a UV interference filter (312 ± 15 nm). The measurements were used to analyze the geometrical characteristics of the flame, i.e. flame length (FL) and height above burner (HAB). All OH*-CL images were acquired with a constant gain of 65%. The gate time was 400 μs . Signal intensity of each flame was analyzed by processing 200 single frames at a 26 Hz repetition rate.

The commercial software Davis 10.2.0 from LaVision was used to analyze the OH*-CL images obtained in this work. The images were corrected for various effects during the analysis. A routine developed by Zanger [30,31], shown schematically in Figure 5 A–B, was used to calculate the flame HAB and FL. The calculation of the HAB was done by determining the flame region (pixels with intensities equal to or greater than 50% of the maximum intensity present in the image) and averaging the height of the boundary pixels in the lower 30% of the flame

region. The FL was calculated in a similar manner to the HAB, but the upper 30% of the flame region was also averaged and the difference between the average of the lower 30% and the average of the upper 30% was calculated (see Figure 5 B).

Figure 5 C shows a red, blue, and green (RGB) color image taken with a Canon EOS 70D digital single lens reflex (SLR) camera using a 55 mm lens for comparison.

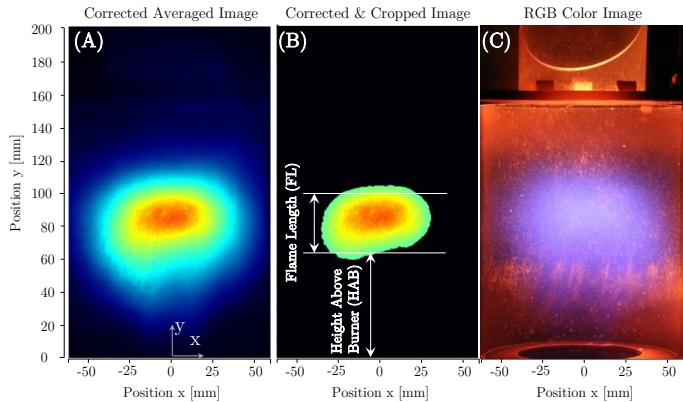


FIGURE 5: A) CORRECTED AND AVERAGED OH*-CL IMAGE, B) ILLUSTRATION OF THE REACTION ZONE WITH REFERENCE TO HAB AND FL LOCATIONS AND C) RGB COLOR IMAGE OF THE FLAME

4.2 Exhaust Gas Emission

An emissions analyzer, ABB: Advanced Optima Process Gas Analyzer AO2000, was used to measure the exhaust gas concentrations for all operating points. All analyzer sensors were calibrated prior to each measurement day. In the exhaust gas section, at a distance of 566 mm from the burner front plate, an exhaust gas composition sampling probe was installed at a single point concentric with the flame tube (Figure 3). The probe was equipped with a coaxial air-cooling system to maintain a constant temperature of 120°C at the probe tip in order to quench further reactions of the probe gas and avoid excessive wall temperatures to cause surface reactions that could distort the gas composition. Hence, it is possible to have defined measuring conditions for all the different operating points of the combustor when measuring exhaust gas.

The gas analyzer can measure water vapor H₂O (Vaisala-HMT330), carbon dioxide CO₂ (ABB Uras26) and oxygen O₂ (ABB Magnos206), as well as carbon monoxide CO (ABB Uras26), unburnt hydrocarbons UHC (ABB MultiFID14 NMHC) and nitrogen oxides NO_x (ABB Limas11). The measurement of O₂, CO and CO₂ is performed under dry conditions, while the measurement of the other species is performed under wet conditions. ABB Gas Analyzer sensor types, ranges and accuracies are listed in Table 2.

A total of 180 readings were taken over 3 minutes (at 1 Hz) for each operating point. The recording of the exhaust gas composition and the OH*-CL images was started after steady-state conditions was reached, meaning that the CO and NO_x emissions did not vary significantly with time. Subsequently, the measurements were time-averaged. The measured moisture and

O₂ content were used to correct the emissions to dry conditions and 15 vol% O₂, respectively.

The UHC measurements were below ABB's UHC measurement accuracy of ±0.37 ppm. For this reason, the possible influence of the characterized factors on the UHC behavior has not been analyzed and was therefore neglected.

The correction of the emissions to a certain percentage of O₂ and to dry conditions is commonly used in gas turbine applications to ensure comparability between different combustor systems. [32]

TABLE 2: ABB PROCESS GAS ANALYZER ACCURACIES AT DIFFERENT RANGES

Species	NO _x	CO
Unit	[ppm]	[ppm]
Sensor	Limas11	Uras26
Range 1	0–10	0–10
Accuracy	±0.10	±0.10
Range 2	0–20	0–100
Accuracy	±0.20	±1
Range 3	0–50	0–200
Accuracy	±0.50	±2

5. BOUNDARY CONDITIONS

In the current study, two separate experiments were designed. First, to characterize the steam effect during superheated injection of Jet A-1. Second, the effect of steam on the combustion behavior of sprayed Jet A-1 injection into the reaction zone. Natural gas was also combusted under the same air equivalence ratios as Jet A-1 to better compare the results with the literature. In addition, the combustion of natural gas and of Jet A-1 can thus be directly assessed and compared with each other.

Initially, water (at 25°C) was injected into the preheated air flow. However, incomplete evaporation of water was observed prior to the combustor even at high air temperature of 305°C with water mass flow rates greater than 1.2 g/s. Therefore, a maximum of WGR = 8% was operable for the superheated injection tests of Jet A-1, in which the level of preheating ΔT was varied from -50 to +50 K (see Section 3). In a next step, water was preheated and injected under superheated conditions to significantly extend the WGR test range. This resulted in the Jet A-1 injecting at spray conditions at $T_{\text{Jet-A1}} = 105^\circ\text{C}$ ($\Delta T = -100\text{ K}$). This was because the electrical preheating was used for the water instead of the liquid fuel heating.

Table 3 gives an overview of the studied combustion parameters and their ranges. The adiabatic flame temperature (T_{ad}) was varied from 1630 to 2385.1 K for Jet A-1 flames which corresponds to air equivalence ratios (λ) of 1 to 2.2. This results in a range of 62 to 143 m/s of bulk velocity (v_{bulk}) at the air nozzle. Due to lower T_{ad} at stoichiometric conditions and lower operating range of NG combustion, the NG T_{ad} ranged from 1684 to 2343.7 K corresponding to $\lambda=1.0$ to 2.0.

The air equivalence ratio, λ , was increased from 1.0 in increments of 0.2 up to the vicinity of the LBO limit for both fuels (see Section 7.1). The WGR was increased in 8% increments from 0 to 16% to measure the effect of steam content on the combustion performance (see Section 7.2). In addition, while keeping the flames of Jet A-1 and NG at stoichiometric condition ($\lambda = 1.0$), the steam content was increased to test the maximum steam loading capability of the flames for both fuels (see Section 7.3). The preheat air temperature was kept constant at $T_{\text{air}} = 305^\circ\text{C}$ for these tests. This was high enough to prevent water condensation in the air tube.

TABLE 3: OVERVIEW OF THE STUDIED COMBUSTION PARAMETERS AND THEIR RANGES

Parameter	Unit	Range
T_{ad}	[K]	1630–2385
(v_{bulk})	[m/s]	62–143
WGR	[%]	0–16
T_{air}	[$^\circ\text{C}$]	305
ΔT	[K]	-100 to +50
P_{th}	[kW _{th}]	22.5
D_{FT}	[mm]	120
D_{AN}	[mm]	16
S_{N}	[-]	0.6

The thermal combustion power (P_{th}) remained constant at 22.5 kW. The flame tube and air nozzle diameters were selected as $D_{\text{FT}} = 120$ mm and $D_{\text{AN}} = 16$ mm, respectively. Jet A-1 and natural gas were selected to evaluate the effect of WGR variation on the combustion performance of liquid and gaseous fuels. The air and water mass flow rates for stoichiometric conditions and the resulting adiabatic flame temperature for NG and Jet A-1 at different WGR levels are shown in Table 4.

TABLE 4: BOUNDARY CONDITIONS OF STEAM INJECTION AT $\lambda = 1.0$

\dot{m}_{air}	$\dot{m}_{\text{H}_2\text{O}}$	WGR	NG T_{ad}	Jet A-1 T_{ad}
[g/s]	[g/s]	[%]	[K]	[K]
7.6	0	0	2343.7	2385.1
7.6	0.66	8	2170.2	2216.4
7.6	1.32	16	1993	2052.5

6. MIXTURES' CHEMICAL-KINETIC PROPERTIES

Laminar flame speed (s_{L}) is the velocity of propagation of the normal flame front relative to the unburned mixture. It is a critical characteristic of a premixed flame because it contains the essential knowledge of the diffusivity and reactivity of a fuel-air mixture [33]. These parameters can vary significantly between different fuels, such as natural gas and Jet A-1, due to differences in chemical composition (see Table 1) and combustion characteristics.

For the fuel-air mixtures in the current study, laminar flame speeds [m/s] were calculated for a range of air equivalence ratios λ from 0.83 to 2.5 at 1 atm. pressure and an air temperature T_{air} of 305°C for Jet A-1 and natural gas at different (WGR = 0–16%) steam contents (see Figure 6 A) using the data in Table 1 and a Cantera code [34]. In addition, ignition delay times [ms]

were calculated for both fuels, three WGR levels and over a wide range of temperature ($T = 909$ – 2000 K) (see Figure 6 B). The kinetic model is based on the Concise mechanism [35], which covers a wide range of C-molecule chemistry and is developed by the DLR Institute of Combustion Technology.

In general, the laminar flame speeds decrease with increasing air-to-fuel ratio, reflecting the reduced reactivity of mixtures at lean-fuel conditions. For Jet A-1, the laminar flame speed seems to be higher than natural gas due to its higher thermal and mass diffusivity [32]. Increasing the steam content of the fuel-air mixture appears to decrease the laminar flame speed. A change from WGR = 0 to 16% causes a 50% decrease in s_{L} at $\lambda = 1.0$. As the mixtures become fuel-leaner, the effect of WGR on s_{L} is reduced.

The increasing reactivity of the mixture with increasing temperature is shown by the constant trend of decreasing ignition delay time for Jet A-1 and NG. The stronger molecular bond of the methane molecule (91.12 mol% of NG), which requires more time to breakdown and oxidize, may account for the longer ignition delay time of NG than Jet A-1. The insensitivity of the ignition delay time at lower steam content is reflected in the negligible increase of the ignition delay time with increasing WGR from 0 to 16% (13 mol%). This behavior seems to be in agreement with that found by Mohapatra et al. [36].

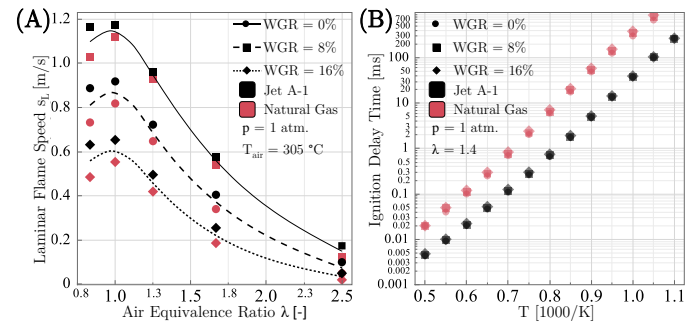


FIGURE 6: (A) LAMINAR FLAME SPEEDS AND (B) IGNITION DELAY TIMES FOR JET A-1 AND NG AT VARIOUS WGR LEVELS AND 1 ATMOSPHERE

The laminar flame speed and ignition delay time values can have a significant effect on the flame length and height above burner. A higher laminar flame speed can result in a shorter flame length and a lower flame height above burner, indicating a more reactive mixture.

7. RESULTS AND DISCUSSION

This section presents and discusses the results of combustion behavior analysis under various steam loads (WGR) for both Jet A-1 and NG flames. Except for the results presented in Section 7.4, where Jet A-1 was preheated from $\Delta T = -50$ to $+50$ K ($T_{\text{Jet A-1}} = 155$ to 255°C), in all experimental results presented in section 7.1 to 7.3, liquid Jet A-1 was injected at $\Delta T = -100$ K ($T_{\text{Jet A-1}} = 105^\circ\text{C}$) and steam at 105 to 115°C .

7.1 Dry Low- NO_x Combustion

The fuel flexibility of the combustor at dry conditions (WGR = 0%) is demonstrated by the wide, stable operating

range and low emission of the combustor for both NG and Jet A-1 (see Figure 7 A and B). The NO_x emissions of Jet A-1 appeared to be higher (+15 ppm) than those of NG at $\lambda = 1$, similar to the results obtained by Snyder et al. [37]. The higher stoichiometric T_{ad} of Jet A-1 and the hot combustion temperatures of the liquid fuel in the vicinity of the droplets may be responsible for this [4].

In contrast to the results of Snyder et al. [37] showing higher NO_x for the liquid fuel at all identical flame temperatures, the results of the current study show nearly equal NO_x and CO values for both fuels at $T_{ad} < 2300$ K. This may be due to similar burning conditions and similar mixing of the two fuels with air in the reaction zone. Another reason for this phenomenon may be the reduced effect of localized near-stoichiometric combustion of the liquid fuel. This approximates the combustion conditions of both liquid and gaseous fuels [3]. The sharp increase in CO levels of NG in the fuel-leaner conditions ($T_{ad} < 1900$ K) is due to the higher T_{ad} at the LBO limit of natural gas and the localized quenching of the reactions leading to increased incomplete combustion.

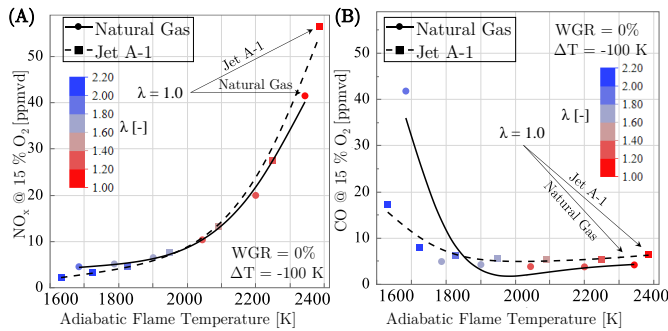


FIGURE 7: (A) NO_x AND (B) CO EMISSIONS FOR JET A-1 AND NG AT WGR = 0%

7.1 Wet Combustion: Exhaust Gas Emissions

The evaluated data in Figure 8 show that increasing the WGR from 0 to 16% reduces the NO_x levels from 56.6 to 10.1 ppm (-82%) for Jet A-1 and from 41.5 to 0 ppm (-100%) for NG at $\lambda = \phi = 1.0$. This is mainly due to thermal effects, namely a reduction in flame temperature from $T_{ad} = 2385$ at WGR = 0% to 2052 K at WGR = 16% for Jet A-1 and $T_{ad} = 2343$ to 1993 K for NG. The chemical effect (kinetics and third body effects), as a result of increasing WGR levels, appears to be dominant in the NO_x formation for liquid Jet A-1 at $T_{ad} > 2100$ K, while for NG the chemical effect is more dominant at $T_{ad} < 2000$ K.

Unlike thermal effects, where the introduction of steam in the reaction zone increases the heat capacity of the mixture and reduces the temperature of the combustion process, chemical effects result from the kinetics of the reaction. The chemical kinetic effect of the presence of steam in the reaction zone can be evaluated by plotting emissions as a function of adiabatic flame temperature, as shown in Figure 8. These chemical effects include both species concentration changes and H_2O third body effects as a result of steam injection.

The actual temperature of the flame can vary depending on the type of fuel being burned (natural gas and Jet A-1), the air equivalent ratio and other factors such as the amount of steam.

This temperature is typically lower than the adiabatic flame temperature, which is the theoretical temperature that would be reached if combustion were perfectly efficient and no heat was lost to the surrounding atmosphere. This adiabatic flame temperature is a function of the enthalpy of combustion of the fuel and the stoichiometry of the reaction.

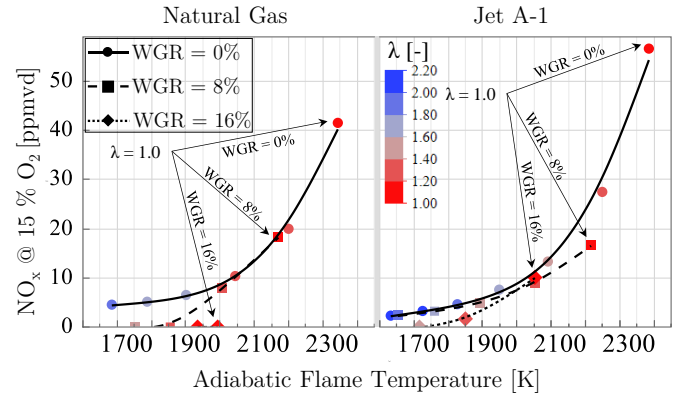


FIGURE 8: NO_x EMISSIONS FOR DIFFERENT T_{ad} , WGR AND FUELS

In addition to the dilution effect of steam injection on the fresh gas and the limitation of oxygen availability, the third body role of water molecules can also promote the formation of free radicals necessary for fuel oxidation. In addition, steam reduces NO_x formation by reducing the formation of oxygen radicals, which are the primary source of NO_x formation, under fuel-lean conditions where O_2 and O radical concentrations are higher. The behavior of NG NO_x emissions is confirmed by Cong et al. [38], who reported that the chemical effect of steam on the formation of NO_x is higher under fuel-lean conditions than under stoichiometric conditions for the combustion of methane. [38]

At WGR = 16%, the stoichiometric operating point for NG measured at $T_{ad} = 1993$ K showed 0 ppm NO_x . For Jet A-1 and the same WGR level, however, the stoichiometric condition ($T_{ad} = 2052$ K) showed 10 ppm NO_x . The unevaporated fuel droplets in the reaction zone of Jet A-1 may account for this difference. Increased formation of local hot pockets and thus increased thermal NO formation can occur due to the presence of fuel droplets in the reaction zone. As the steam content reduced to WGR = 8%, the 0 ppm NO_x emissions shifted to lower T_{ad} levels for NG flames. There was no measurable difference in NO_x levels at $T_{ad} = 2052$ K for either WGR levels for Jet A-1 flames. The reduction of NO_x emissions by increasing steam concentration is mainly caused by the reduced flame temperature, which leads to reduced thermal NO formation rate. Other factors influencing this behavior are dilution and reduction of N_2 concentration [162].

The measured CO emission levels of the corresponding operating points with WGR variation for Jet A-1 and NG are shown in Figure 9. For all WGR levels for Jet A-1 at stoichiometric conditions, the CO levels remain constant at 5.8 ± 0.74 ppm. At lower flame temperatures of $T_{ad} < 1700$ K, CO levels increase to a maximum of 17.3 ppm at WGR = 0% due to flame quenching effects near the LBO limit. Note the T_{ad}

LBO limit of NG was observed to be higher than Jet A-1 (see Section 7.3).

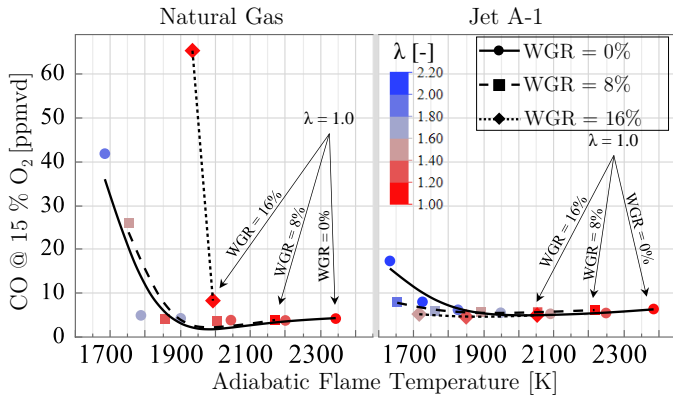


FIGURE 9: CO EMISSIONS FOR DIFFERENT T_{ad} , WGR AND FUELS

The emitted CO concentrations are not significantly affected by WGR = 0–8% for the natural gas flames. However, at WGR = 16%, the operating points at T_{ad} = 1993 and 1935 K have the largest deviation in CO levels of +5 and +61 ppm due to the proximity of the T_{ad} LBO limit. Here, low flame temperatures and local reaction zone quenching prevent CO oxidation to CO_2 . In contrast to the CO values reported in the literature [39] for a steam injected premixed swirl stabilized combustor operated with NG, the CO values measured in this study remain constant over a wide operating range.

7.2 Wet Combustion: Flame Shape

Figure 10 A and B show the time-averaged OH^* images for different steam loads for the Jet A-1 and NG, respectively, representing the heat release zones. The effect of mixing the fuel and air prior to the reaction zone is the same for both dry and wet conditions due to the identical air equivalence ratios and the slightly increased bulk velocities as a result of WGR increase (rows: left to right). The flame temperature (shown above each OH^* image) decreases with increasing air equivalence ratio λ (columns: bottom to top). Note, that visual analysis of the OH^* images showed that the macro software used to evaluate the OH^* data could not adequately assess the contour of the reaction zone due to the very low intensity of the NG flames' OH^* signal at higher WGR levels. Therefore, the interpretation of the data should be made with caution.

Increasing the steam content in the Jet A-1 and air mixture results in a wider and less concentrated reaction zone at $\lambda = 1.0$ from WGR = 0 to 16%. This is due to the lower flame temperature (2385 to 2052 K) and the increase in bulk velocity (66.9 to 78.5 m/s) caused by the injection of steam. Higher WGR conditions cause the reaction rates (reactivity) and the flame velocity to decrease (see Figure 6 A). This results in a slight shift of the reaction zone downstream of the flow and its further propagation in the direction of the flame tube walls. The air equivalence ratio λ must be reduced to maintain the same adiabatic flame temperature as the WGR increases. Therefore, an approximately similar T_{ad} can be obtained by viewing the images

diagonally (figures from top left to bottom right). Thus, as the WGR increases, the OH^* images can be compared with similar T_{ad} values.

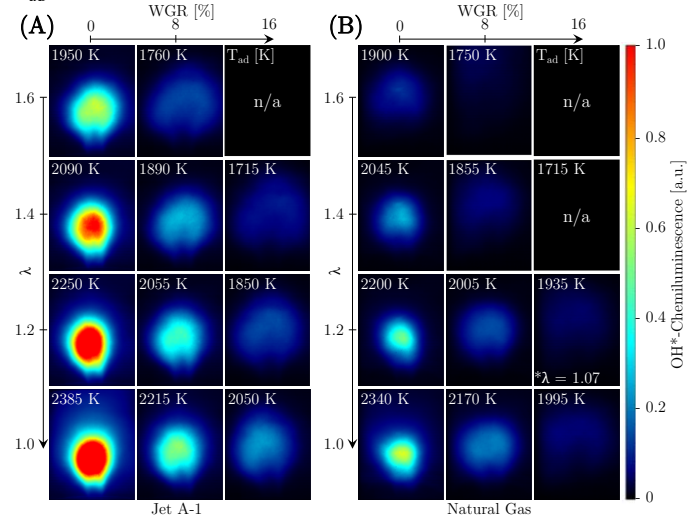


FIGURE 10: OH^* IMAGE MATRIX AT DIFFERENT λ AND WGR FOR (A) JET A-1 AND (B) NATURAL GAS

The influence of water injection on the heat release zone at a constant adiabatic flame temperature was investigated by Lellek et al. [40] using NG as fuel. Their results showed that when water was injected, there was almost no change in the shape or intensity of the heat release zone. In contrast, the presently measured OH^* signal intensities for NG and Jet A-1 are more volumetric and significantly reduced at similar T_{ad} (max. ± 60 K) with increasing WGR levels. This is in agreement with the results of Göke [39] and proves that a suppression of excited OH radicals formation (in addition to the thermal effects due to the $T_{ad} \pm 60$ K difference) occurs at similar T_{ad} and decreasing air equivalence ratio.

The concentration of O_2 in the fresh gas is lower for higher values of WGR. The result is a decrease in the reactivity of the mixture. This leads to the reactions becoming slower and thus less heat is released. Local effects such as mixing can also play an important role. Another factor that may play a role is the bulk velocity increase and the associated mixing effects between fresh gas and exhaust gas.

The main reasons for the difference in flame intensity between Jet A-1 and NG are the fuel phase in which they are injected into the reaction zone and their different chemical compositions. The high-intensity zones of Jet A-1 flames are in part due to locally fuel-rich regions where rapid evaporation and combustion of fuel droplets occur. It may also be influenced by mixing effects after fuel injection, as the gaseous fuel mixes with the air-steam flow in a different way than the Jet A-1 spray does.

Flame Height Above Burner (HAB) for the measured operating points at various WGR levels is shown in Figure 11. The HAB values from WGR = 0 to 8% remain similar with a maximum deviation of 7 mm over the entire T_{ad} range for both Jet A-1 and NG fuel. These HAB values increase slightly with decreasing adiabatic flame temperature due to decreased reactivity of the mixture at fuel-leaner conditions. In addition, at

WGR = 16%, due to the lower flame speed and reactivity of the mixture, the HAB values increase by a maximum of 10.7 mm for Jet A-1 and 26.5 mm for NG. The marginal effect of WGR = 8% for both NG and Jet A-1 could be due to insignificant concentration of added steam in the reaction zone, which leads to its reduced effect on the flame HAB behavior. Thermal effects are responsible for the decrease in flame speed of hydrocarbon flames [38,41,42].

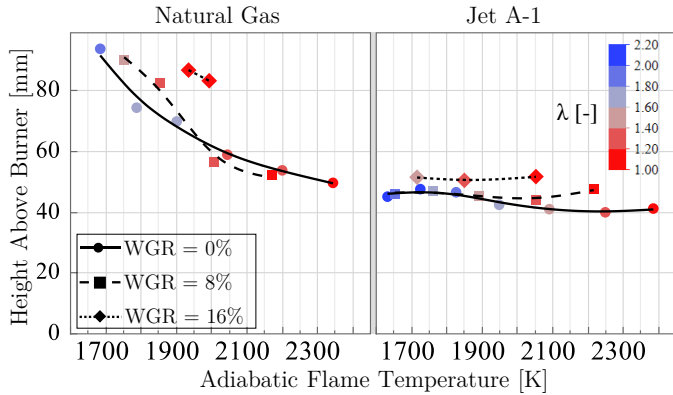


FIGURE 11: HAB FOR DIFFERENT T_{ad} , WGR AND FUELS

Due to the higher reactive nature of Jet A-1, its ignition delay time is reduced (see Figure 6 B), causing the pre-mixed Jet A-1 and air to ignite faster, resulting in a shorter HAB. Jet A-1 HAB levels remain mostly constant over the tested T_{ad} levels due to the much larger operating range of Jet A-1 compared to NG flames. With decreasing T_{ad} , natural gas HABs increase significantly. It appears that due to the presence of hot burning fuel droplets, the Jet A-1 flames maintain a similar level of reactivity.

Figure 12 shows the flame length data derived from the averaged OH* images for different levels of WGR for both Jet A-1 and NG. At all WGR levels, the flame lengths for both fuels increase with decreasing T_{ad} due to the increased bulk velocities at higher air equivalence ratios λ . The lower global reactivity of the fuel-air mixture and shorter residence times for fuel-leaner conditions contribute to slower evaporation of the Jet A-1 droplets in the reaction zone.

It appears that, as T_{ad} levels decrease, the flame lengths of Jet A-1 become increasingly insensitive to WGR values, similar to the HAB behavior of Jet A-1. An analysis of the FL values in relation to the air equivalence ratio λ showed a clear increase in FL with increase in WGR for all λ values (data not shown here). This indicates that the level of adiabatic flame temperature determines the FL values rather than WGR.

Increasing the WGR values from 0 to 8 and 16% at $T_{ad} = 2050$ K results in a consistent increase in FL for Jet A-1 flames from 44, 48.8, and 55.8 mm, respectively. This range of 11.8 mm decreases to an overall increase of 1.2 mm at fuel-lean conditions due to the reduced chemical kinetic effect and increased fuel atomization quality. The trailing and leading edges of the swirler vanes have proved to enhance fuel atomization with increasing bulk velocity in the combustor mixing channel.

The FL for NG flames at WGR = 0% shows increasing values with decreasing T_{ad} levels due to the increase in bulk velocity and the decrease in residence time. This is as expected. However, there is no consistent trend for their FL values at WGR = 8–16% due to the previously mentioned issues with evaluating low OH* intensity of NG at higher WGR levels.

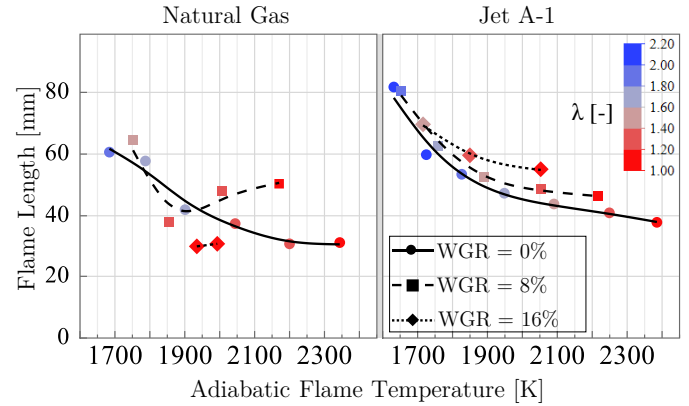


FIGURE 12: FL FOR DIFFERENT T_{ad} , WGR AND FUELS

7.3 Combustor Maximum Steam Injection Capability

A flame's Lean Blow Out (LBO) limit is defined as the point at which the air-fuel mixture becomes too lean (insufficient fuel) to sustain combustion, causing the flame to blow out. This LBO limit can be expressed in terms of the adiabatic flame temperature that represents the lowest possible T_{ad} at which the flame can be maintained (T_{ad} LBO limit).

The T_{ad} LBO limits (y-axis) for both Jet A-1 and NG are plotted against WGR (x-axis) in Figure 13 A. For comparison, Figure 13 B shows the air equivalence ratio λ (y-axis) plotted for the same WGR values. For the LBO tests, at a constant thermal power (fuel mass flow) of 22.5 kW, the air mass flow rate was increased by 0.02 g/s ($\Delta T_{ad} \approx -2$ K per second). At the same time, the water mass flow rate was adjusted as the air mass flow rate increased to keep the WGR at a constant level. The T_{ad} LBO limits were approached three times for each WGR level to gain statistical confidence. Note that in order to avoid large intakes of unburned Jet A-1 during flameout events, no exhaust gas measurement was performed during the LBO tests.

The more gradual slope of the Jet A-1 T_{ad} LBO limits with increasing WGR compared to the NG LBO limits with a much steeper slope (see Figure 13 A) indicates different combustion characteristics of the fuels and their interactions with steam. Pathania et al. [43] investigated and compared the LBO limits of pre-vaporized kerosene flames with those of methane flames. The authors found that the low temperature reactions were more prominent in the Jet A flame than in the methane flame. Using the CH₂O-PLIF measurement technique, a slightly higher intensity of CH₂O was observed in Jet A flames than in methane flames. This higher intensity caused the CH₂O to mix with new reactants in the recirculation zone, possibly resulting in a more stable Jet A flame.

The maximum WGR content at $\lambda = 1$ was found to be $\text{WGR} \approx 32\%$ ($T_{\text{ad}} \approx 1688 \text{ K}$) for Jet A-1 and $\text{WGR} \approx 21\%$ ($T_{\text{ad}} \approx 1895 \text{ K}$) for NG. Both thermal and chemical effects of steam injection may be responsible for the relatively smaller operating range of the NG flame at the same WGR level, as shown in Figure 13 B. Increasing WGR appears to have a more significant effect on the combustion of natural gas than it does on the Jet A-1 flame, which contains fuel droplets that may burn at near stoichiometric levels and help to sustain the chain reaction in the combustion process.

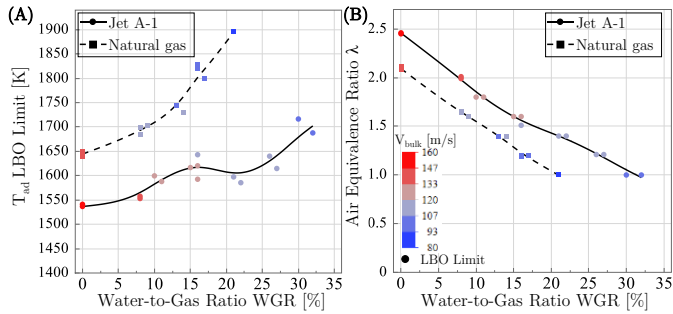


FIGURE 13: OPERATING RANGE FOR (A) T_{ad} LBO LIMITS AND (B) λ FOR VARIOUS WGR LEVELS

At $\text{WGR} = 16\%$, the natural gas flames showed a T_{ad} LBO limit of 1830 K while Jet A-1 flames remained stable until T_{ad} LBO of 1620 K. To maintain a stable flame as the WGR increases, the air equivalence ratio must be reduced. The concentration of OH radicals increases as the fresh gas mixture becomes fuel-richer. The result is an increased global rate of reaction and higher flame speed [44]. Under dry conditions, Jet A-1 flame had a mean T_{ad} LBO limit of $1538 \pm 2.5 \text{ K}$, 107 K lower than NG flame. This is due to the fuels' chemical composition and difference in fuel phase. For example, methane, the main component (91.12 mol%) of the tested natural gas, requires a higher temperature for cracking and participation in the combustion process due to its stronger molecular bonding than other long-chain hydrocarbon fuels.

7.4 Liquid Fuel Superheated Injection

Combustion emission data collected during superheated injection of Jet A-1 while injecting water at 25°C into the preheated airflow are presented in this section. Operation with a maximum $\text{WGR} = 8\%$ was possible due to the technical limitations described in section 5. It remains uncertain, whether the entire amount of injected water also reached the plenum and then the combustion chamber or partially remained in the air-water mixing channel.

The effect of sprayed and prevaporized Jet A-1 on the combustion performance at dry and wet conditions is shown in Figure 14. The graphs show the NO_x and CO emissions for various $\Delta T = -50$ to $+50 \text{ K}$. At $\Delta T = -50 \text{ K}$ ($T_{\text{fuel}} = 155^\circ\text{C}$), the Jet A-1 is atomized via mechanical breakup and disintegration of the swirling and fast liquid fuel sheet. At $\Delta T = 0 \text{ K}$ ($T_{\text{fuel}} = 205^\circ\text{C}$), the injected fuel is at its saturation temperature. At this condition, the fuel transitions into superheated injection regime and is atomized by a mix of both mechanical and thermal

breakup. In the superheated regime, at $\Delta T = +50 \text{ K}$ ($T_{\text{fuel}} = 255^\circ\text{C}$), the typical fuel spray is replaced by a plume of a narrow rapidly evaporating and axially accelerating fuel with significantly reduced radial penetration.

The NO_x (left y-axis) and CO (right y-axis) emissions are represented by the black and red curves, respectively. Due to increased thermal NO formation, NO_x emissions increase exponentially with increasing T_{ad} . For all ΔT levels, there is virtually no difference in NO_x levels at $\text{WGR} = 0$ and 8% . This is an indication that for this combustor design, the state of entry of Jet A-1 into the reaction zone has a negligible effect on NO_x emissions. Furthermore, only the adiabatic flame temperature is reduced by the addition of steam to the fresh gas mixture. There is no change in the NO_x levels as a result of the chemical effects.

It is interesting to note that at $\Delta T = -50 \text{ K}$, $\text{WGR} = 8\%$ and $T_{\text{ad}} = 2222 \text{ K}$, the measured NO_x emission is 28.9 ppm. Under the same conditions, but at $\Delta T = -100 \text{ K}$ (see Figure 8), the NO_x level is 16.7 ppm. This relatively large discrepancy could be due to two possible reasons. The first is the 50 K difference in the preheat temperature of Jet A-1 and the possible effect on the spray characteristics of the fuel. Second, the possibility that not all of the injected water reached the combustion zone, while some water remained in the air lines. The latter seems to be more plausible. Injecting Jet A-1 at a lower temperature ($\Delta T = -100 \text{ K}$) cannot lead to such a reduction in NO_x levels, as demonstrated by [18]. If only a portion of the injected water reached the reaction zone, then the actual WGR would have been lower, resulting in a reduction in the effect of the steam on the emissions.

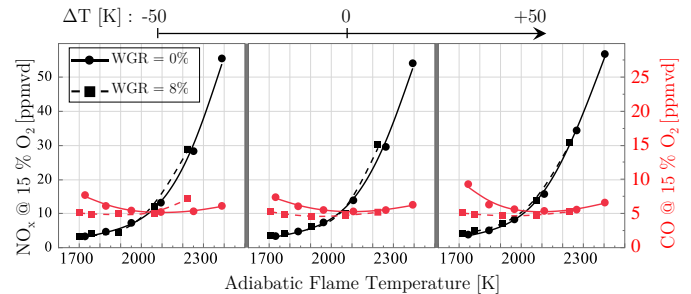


FIGURE 14: NO_x AND CO EMISSIONS OF JET A-1 COMBUSTION AT DIFFERENT ΔT AT WGR LEVELS

Towards the LBO limit of the flame, the CO emissions of $\text{WGR} = 8\%$ show lower levels than $\text{WGR} = 0\%$. This behavior is in agreement with the effect of the steam on the CO emissions that was previously discussed in section 7.1. At $\Delta T = +50 \text{ K}$ and $\text{WGR} = 0\%$, both the NO_x and CO levels appear to be higher than at $\Delta T = -50$ and 0 K , respectively, due to the superheated injection effect of Jet A-1. Superheated injection not only causes liquid fuel to vaporize, but also causes it to expand rapidly in the axial direction and penetrate less in the radial direction. While fuel evaporation should lead to better fuel-air mixing, the latter two effects reduce fuel-air mixing and lead to hot spots and increased incomplete combustion within the reaction zone, which tends to form higher NO_x levels. In addition, CO levels

may increase as a result of the reduced fuel-air mixing due to superheated injection.

At WGR = 8%, the NO_x and CO emissions remain mostly constant for different ΔT levels throughout the tested T_{ad} range of 1700-2389 K. It appears that the injected steam has counteracted the influence of the superheated injection ($\Delta T = +50$ K) of the liquid fuel by minimizing the hot spots. As for the lower CO levels at wet combustion, the increase in H₂O concentration in the reaction zone as a result of steam injection leads to increased concentration of OH radicals, which results in the oxidation of CO to CO₂ [38].

As shown in section 7.2, the effect of steam injection on HAB and FL as a function of T_{ad} variation was negligible. The effect of ΔT on the flame shape structure was also very small. This is in agreement with the results obtained by [18] for the swirl-assisted jet-stabilized combustor.

8. SUMMARY AND CONCLUSION

Steam injection is an alternative method of diluting the reactant mixture and reducing the flame temperature. The flame temperature is reduced mainly due to the thermal effect of the steam acting as a heat sink. Compared to the dry combustion, steam injection has the advantage that the velocity profile is not significantly disturbed and thus the performance of the combustion stability can be maintained.

Using steam as an external perturbation into the swirl-assisted jet-stabilized combustor minimized NO_x emissions by reducing the adiabatic flame temperature for both Jet A-1 and NG combustion. However, at constant T_{ad}, some reduction in NO_x emissions was also observed. This was due to chemical kinetics and third body effects. Under stoichiometric conditions $\lambda = 1.0$, the NO_x emission was reduced by -82% and -100%, respectively, with increasing WGR = 0 to 16% for the Jet A-1 and NG combustion. There was little effect on CO emissions by increasing the steam content. The heat release zone became more volumetric, while its intensity (OH*) decreased with increasing WGR even at similar T_{ad} values.

For Jet A-1 and NG, there was no significant change in HAB levels as the WGR increased from 0 to 8%. The HAB values only increased at the highest WGR level (16%) for both fuels. Since the adiabatic flame temperature played a more dominant role in changing the shape of the reaction zone, the flame length of Jet A-1 showed a minimal change with increasing WGR at T_{ad} < 1900 K. During the entire dry and wet experiments, no sign of thermoacoustic instability was observed for neither of the tested fuels and WGR levels.

Compared to NG flames, the operating range of Jet A-1 flames decreased with a lesser LBO limit T_{ad} slope as WGR increased. This indicated that even under wet conditions, the influence of the combustion characteristics of Jet A-1 and NG, local mixing, and the presence of fuel droplets on extending the operating range was significant. The maximum steam content at which a flame was still operational was found at WGR \approx 32% and WGR \approx 21% for Jet A-1 and NG, respectively.

Steam injection can have several effects on a GT engine combustor application. In particular, it can have an effect on

emissions and operating range. While operating the GT combustor at a similar turbine inlet temperature, steam injection can reduce NO_x emissions. It can also result in heat absorption and a reduction in peak temperature. This can have the effect of extending liner life. It is also possible to increase the part load operating range of the GT. This is achieved by allowing the GT to operate at a higher power setting without exceeding the temperature limits imposed by the liner wall and turbine blades. This can be particularly useful in hot and dry environments where the combustor inlet temperature is higher, thus limiting the engine to operate at higher loads.

The added engineering and operational considerations also need to be taken into account. For example, the additional steam injection system, the potential effects of steam on GT components due to increased moisture content, and its effect on overall system complexity. Therefore, a complete cost-benefit analysis must be performed before the design or redesign of a GT combustion system.

ACKNOWLEDGMENT

The efforts of Stefan Fiedler and Timo Wagner are greatly appreciated for their support throughout the testing campaign. Special thanks to the VT-DLR workshop, Jens Kreeb, Ralph Bruhn, Sven Schober and Michael Gröninger for their efforts in manufacturing the combustor components. This research is funded by the German Aerospace Center (DLR e. V.) as an internal project.

9. REFERENCES

- [1] Krill W. V., Kesselring J. P., and Chu E. K., 1979, "Catalytic Combustion for Gas Turbine Applications,"
- [2] Davis L. B., and Washam R. M., 1989. *Development of a Dry Low NO_x Combustor*.
- [3] Lefebvre A. H., and Ballal D. R., 2010. *Gas Turbine Combustion*, CRC Press: Taylor & Francis Group, Boca Raton, FL.
- [4] Shen Y., Ghulam M., Zhang K., Gutmark E., and Duwig C., 2020, "Vortex breakdown of the swirling flow in a Lean Direct Injection burner," *Physics of Fluids*, **32**, p. 125118.
- [5] Marek C. J., Smith T. D., and Kundu K., 2005, "Low emission hydrogen combustors for gas turbines using Lean Direct Injection," *41st AIAA/ASME/SAE/ASEE Joint Propulsion Conference & Exhibit*, American Institute of Aeronautics and Astronautics, Reston, Virginia.
- [6] Behrendt T., Heinze J., and Hassa C., Eds., 2003. *Experimental Investigation of a New LPP Injector Concept for Aero Engines at Elevated Pressures*.
- [7] Nakamura S., McDonell V., and Samuelsen G. S., 2008, "The Effect of Liquid-Fuel Preparation on Gas Turbine Emissions," *Journal of Engineering for Gas Turbines and Power*, **130**(021506), pp. 1–11.
- [8] Hatch M., Sowa W., Samuelsen G., and Holdeman J., 1995, "Influence of Geometry and Flow Variations on NO Formation in the Quick Mixer of a Staged Combustor,"
- [9] Jeong G., and Ahn K., 2021, "One-Dimensional Analysis of Double Annular Combustor for Reducing Harmful Emissions," *Energies*, **14**, p. 3930.
- [10] Mongia H., 2003. *TAPS: A Fourth Generation Propulsion Combustor Technology for Low Emissions*.
- [11] Marian Hiestermann, Marco Konle, and Ludovic de Guillebon, 2022, "NUMERICAL INVESTIGATION OF THE EFFECT OF

HIGH STEAM LOADS ON THE COMBUSTION OF AN ACADEMIC PREMIXED SWIRL STABILIZED COMBUSTOR,” Proceedings of Global Power & Propulsion Society.

- [12] Roointon Pavri, and Gerald D. Moore, 2001, “Gas Turbine Emissions and Control: GE Energy Services: GER-4211,”
- [13] Kaiser S., Schmitz O., Ziegler P., and Klingels H., 2022, “The Water-Enhanced Turbofan as Enabler for Climate-Neutral Aviation,” *Applied Sciences*, **12**(23), p. 12431.
- [14] Marcellan A., Henke M., Schuldt S., Maas P., and Göhler-Stroh A., A numerical investigation of the Water-Enhanced Turbofan A numerical investigation of the Water-Enhanced Turbofan laboratory-scale ground demonstrator, *AIAA SciTech Forum 2022*.
- [15] Matthew J. Degges, J. Eric Boyer, Kenneth K. Kuo, and Luca Basini, 2010, “Influence of steam on the flammability limits of premixed natural gas/oxygen/steam mixtures,” *Chemical Engineering Journal*, **165**(2), pp. 633–638.
- [16] Lefebvre A. H., Ed., 1995. *The Role of Fuel Preparation in Low Emissions Combustion*.
- [17] Izadi S., Zanger J., Baggio M., Seliger-Ost H., Kutne P., and Aigner M., 2024, “Experimental Investigation of the Effect of Superheated Liquid Fuel Injection On the Combustion Characteristics of Lean Premixed Flames,” *ASME. J. Eng. Gas Turbines Power*(146), pp. 1–13.
- [18] Izadi S., Zanger J., Seliger-Ost H., Kutne P., and Aigner M., 2024, “Experimental Evaluation of Combustor Configuration's Impact on a Swirl-Assisted Jet-Stabilized Combustor Performance,” Proceedings of the ASME Turbo Expo 2024: Turbomachinery Technical Conference and Exposition. Volume 3A: Combustion, Fuels, and Emissions.(GT2024-127693).
- [19] Izadi S., Seliger-Ost H., Zanger J., Kutne P., and Aigner M., 2024, “Analysis of Liquid Fuel Effect on Swirl-Assisted Jet-Stabilized Combustor Performance,” Proceedings of the ASME Turbo Expo 2024: Turbomachinery Technical Conference and Exposition. Volume 3A: Combustion, Fuels, and Emissions.(GT2024-127721).
- [20] Kathrotia T., Oßwald P., Zinsmeister J., Methling T., and Köhler M., 2021, “Combustion kinetics of alternative jet fuels, Part-III: Fuel modeling and surrogate strategy,” *Fuel*, **302**, p. 120737.
- [21] Lefebvre A. H., and McDonell V. G., 2017. *Atomization and sprays*, CRC Press Taylor & Francis Group, Boca Raton, London, New York.
- [22] W Yang W. B., Ed., 2003. *Effects of fuel temperature and flame locations on emissions of nitrogen oxides in combustion with high temperature air*.
- [23] Yin Z., Kutne P., Eichhorn J., and Meier W., 2021, “Experimental Investigations of Superheated and Supercritical Injections of Liquid Fuels,” *Journal of Engineering for Gas Turbines and Power*, **143**(4).
- [24] Grazia Lamanna, Hend Kamoun, Bernhard Weigand, and Johan Steelant, 2014, “Towards a unified treatment of fully flashing sprays,” *International Journal of Multiphase Flow*, **58**, pp. 168–184.
- [25] Rachner M., 1998. *Die Stoffeigenschaften von Kerosin Jet A-1*, DLR, Abt. Unternehmensorganisation und -information.
- [26] Reid Robert C., Prausnitz John M., and Poling Bruce E., 1987, “The properties of gases and liquids,” *Journal of Women's Health*.
- [27] Leo M. de, Saveliev A., Kennedy L. A., and Zelepouga S. A., 2007, “OH and CH luminescence in opposed flow methane oxy-flames,” *Combustion and Flame*, **149**(4), pp. 435–447.
- [28] Kathrotia T., 2011, “Reaction Kinetics Modeling of OH(*), CH(*), and C2(*) Chemiluminescence,” Heidelberg, Ruprecht-Karls-Universität.
- [29] Tinaut F. V., Reyes M., Giménez B., and Pastor J. V., 2011, “Measurements of OH* and CH* Chemiluminescence in Premixed Flames in a Constant Volume Combustion Bomb under Autoignition Conditions,” *Energy & Fuels*, **25**(1), pp. 119–129.
- [30] Zanger J., 2016, “Experimentelle Charakterisierung eines atmosphärisch betriebenen, jet-stabilisierten Mikrogasturbinenbrenners für Erdgas,” Stuttgart, Universität.
- [31] Bower H. E., Schwärzle A., Grimm F., Zornek T., and Kutne P., 2019, “Experimental Analysis of a Micro Gas Turbine Combustor Optimized for Flexible Operation with Various Gaseous Fuel Compositions,” *Journal of Engineering for Gas Turbines and Power*, **142**(031015), pp. 1–9.
- [32] Turns S. R., 2012. *An Introduction to Combustion: Concepts and Applications*, McGraw-Hill.
- [33] Chong C. T., and Ng J.-H., 2021. *Biojet Fuel in Aviation Applications: Production, Usage and Impact of Biofuels*, Elsevier.
- [34] David G. Goodwin and Harry K. Moffat and Ingmar Schoegl and Raymond L. Speth and Bryan W. Weber, 2023, “Cantera: An Object-oriented Software Toolkit for Chemical, <https://www.cantera.org>, 10.5281/zenodo.8137090,”
- [35] Kathrotia T., Oßwald P., Naumann C., Richter S., and Köhler M., 2021, “Combustion kinetics of alternative jet fuels, Part-II: Reaction model for fuel surrogate,” *Fuel*, **302**, p. 120736.
- [36] Mohapatra S., Mohapatro M. B., Pasha A., Alsulami R., Dash S., and Reddy V., 2022, “Adaptability of different mechanisms and kinetic study of methane combustion in steam diluted environments,” *Scientific Reports*, **12**, p. 4577.
- [37] Snyder T. S., Rosfjord T. J., McVey J. B., and Chiappetta L. M., Eds., 1994. *Comparison of Liquid Fuel/Air Mixing and NOx Emissions for a Tangential Entry Nozzle*.
- [38] Le Cong T., and Dagaut P., 2009, “Experimental and detailed modeling study of the effect of water vapor on the kinetics of combustion of hydrogen and natural gas, impact on NO x,” *Energy & Fuels*, **23**(2), pp. 725–734.
- [39] Göke S., 2012, “Ultra Wet Combustion: An Experimental and Numerical Study,”
- [40] Lellek S., and Sattelmayer T., 2015, “Influence of Water Injection on Heat Release Distribution, Lean Blowout and Emissions of a Premixed Swirl Flame in a Tubular Combustor,”
- [41] Müller-Dethlefs K., and af Schlader, 1976, “The effect of steam on flame temperature, burning velocity and carbon formation in hydrocarbon flames,” *Combustion and Flame*, **27**, pp. 205–215.
- [42] Babkin V. S., and V'yun A. V., 1971, “Effect of water vapor on the normal burning velocity of a methane-air mixture at high pressures,” *Combustion, Explosion and Shock Waves*, **7**(3), pp. 339–341.
- [43] Pathania R. S., Helou I. E., Skiba A. W., Ciardiello R., and Mastorakos E., 2023, “Lean blow-off of premixed swirl-stabilised flames with vapourised kerosene,” Proceedings of the Combustion Institute, **39**(2), pp. 2229–2238.
- [44] Griebel P., Boschek E., and Jansohn P., 2006, “Lean Blowout Limits and NOx Emissions of Turbulent, Lean Premixed, Hydrogen-Enriched Methane/Air Flames at High Pressure,” *0742-4795*, **129**(2), pp. 404–410.